# Expanding the Polymethine Paradigm: Evidence for the Contribution of a Bis-Dipolar Electronic Structure

**ARTICLE** *in* THE JOURNAL OF PHYSICAL CHEMISTRY A · MAY 2014

Impact Factor: 2.69 · DOI: 10.1021/jp501358q · Source: PubMed



**8 AUTHORS**, INCLUDING:

Denis Jacquemin
University of Nantes
**356** PUBLICATIONS **8,265** CITATIONS
SEE PROFILE

Boris Le Guennic
Université de Rennes 1
**137** PUBLICATIONS **2,367** CITATIONS
SEE PROFILE

Chantal Andraud
Claude Bernard University Lyon 1
**222** PUBLICATIONS **3,040** CITATIONS
SEE PROFILE

Olivier Maury
Ecole normale supérieure de Lyon
**169** PUBLICATIONS **3,431** CITATIONS
SEE PROFILE

THE JOURNAL OF PHYSICAL CHEMISTRY A

Article

pubs.acs.org/JPCA

# Expanding the Polymethine Paradigm: Evidence for the Contribution of a Bis-Dipolar Electronic Structure

Simon Pascal,[†] Alexandre Haefele,[†] Cyrille Monnereau,[†] Azzam Charaf-Eddin,[§] Denis Jacquemin,[§,∥] Boris Le Guennic,*[,‡] Chantal Andraud,*[,†] and Olivier Maury*[,†]

[†]Laboratoire de Chimie, UMR 5182, CNRS, ENS Lyon, Université Lyon 1, 46 Allée d'Italie, 69364 Lyon Cedex 07, France

[‡]Institut des Sciences Chimiques de Rennes, UMR 6226 CNRS, Université de Rennes 1, 263 Avenue du Général Leclerc, 35042 Rennes Cedex, France

[§]Laboratoire CEISAM, CNRS 6230, Université de Nantes, 2 Rue de la Houssinière, BP 92208, 44322 Nantes Cedex 3, France

[∥]Institut Universitaire de France, 103 Bd Michelet, 75005 Paris Cedex 5, France

Supporting Information

**ABSTRACT:** Although it has been reported in a few instances that the spectroscopic properties of cyanine dyes were strongly dependent on the nature of the chemical substitution of their central carbon atom, there has not been to date any systematic study specifically aimed at rationalizing this behavior. In this article, such a systematic study is carried out on an extended family of 17 polymethine dyes carrying different substituents on their central carbon, some of those being specifically synthesized for this study, some of those similar to previously reported compounds, for the sake of comparison. Their absorption properties, which spread over the whole visible to near-infrared spectral range, are seen to be dramatically dependent on the electron-donating character of this central substituent. By correlating this behavior to NMR spectroscopy and (vibronic) TD-DFT calculations, we show that it results from a profound modification of the ground state electronic configuration, namely, a progressive localization of the cationic charge on the central carbon as the electron-donating nature of the central substituent is increased.

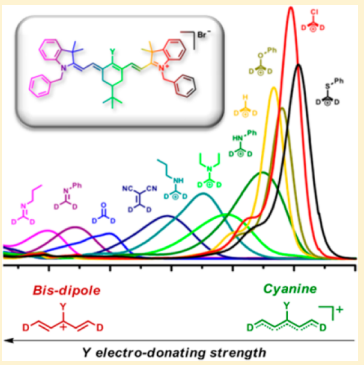


## INTRODUCTION

Old polymethine dyes, discovered in the middle of the 19th century for photography applications, continue to hold a real fascination in the scientific community owing to their unique spectroscopic properties.[1−5] In the past decade, these dyes found a renewal of interest for near-infrared (NIR) applications in biological imaging[6,7] or for the design of advanced photonic materials (laser dyes, nonlinear optics...).[1−5,8,9] Generally speaking, polymethine dyes are charged compounds where the positive (respectively negative) charge is delocalized between two electron-donating (respectively withdrawing) groups via an odd number of $sp^2$ carbon atoms.[1,2,10] In spite of their wide range of use, the complete rationalization of their very particular photophysical properties remains a matter of debate from both experimental and theoretical points of view.

Recently, by analogy with quadupolar dye,[11] Van Stryland and co-workers proposed to rationalize the spectroscopic properties of polymethine dyes on the basis of three electronic states: a doubly degenerated dipole state where the charge is localized on one extremity and a charge-centered state.[12] The relative energies of the three states determine the nature of the ground state and consequently the spectral properties of the dyes. This approach explained the different behaviors observed in solution that correspond to different ground state electronic configurations:

(i) The cyanine configuration, introduced by Dähne in the early 1970s,[13,14] corresponds to a strong mixture of the three aforementioned states (form I, Figure 1). Consequently the charge is fully delocalized in a symmetric way over the entire conjugated backbone and the bond-length alternation (BLA) is negligible.[15] This cyanine electronic structure is characterized by a sharp, exceptionally intense absorption, located for heptamethines in the NIR spectral range with a vibronic shoulder at higher energy.

(ii) The dipolar configuration (form II, Figure 1), where the charge is predominantly localized at one extremity, results in both ground state symmetry breaking and a positive BLA. This dipolar electronic structure is characterized by a broad, structureless charge transfer type transition that is blue-shifted compared to the cyanine one. It is possible to change the contribution of each electronic configuration, in other words to "cross the cyanine limit" (I → II), by increasing the chain length of the conjugated skeleton as in the pioneering works of Brooker[16] and Tolbert,[17] by increasing the solvent polarity,[18,19] or by the ion-pairing effect.[20,21] On the

Received: February 7, 2014
Revised: May 16, 2014
Published: May 16, 2014





dx.doi.org/10.1021/jp501358q | J. Phys. Chem. A 2014, 118, 4038−4047

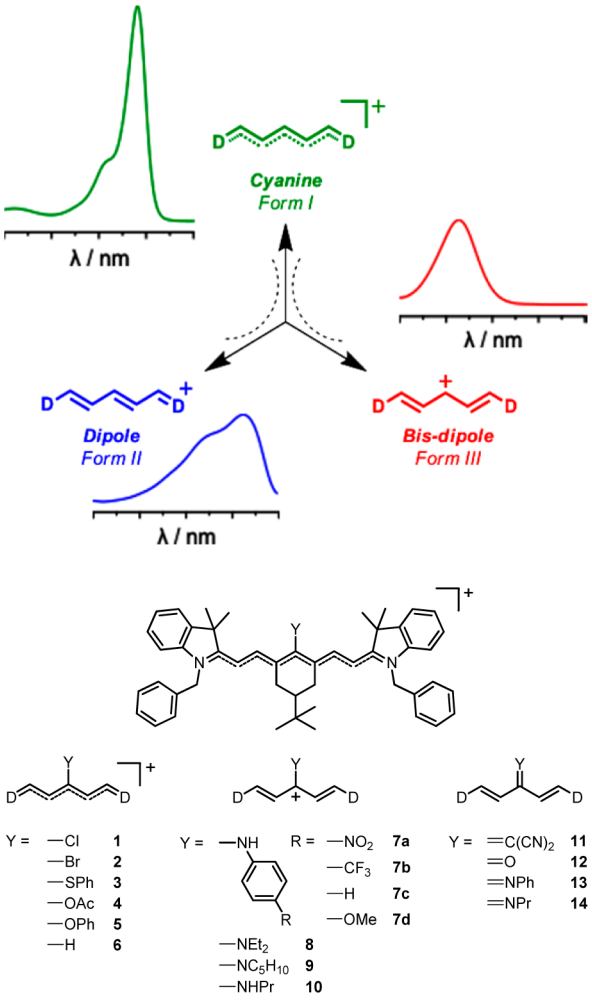


**Figure 1.** (Top) Three electronic configurations of polymethine dyes and their respective absorption profiles and (bottom) structures of the heptamethine dyes involved in this study.

other hand, Würthner and co-workers demonstrated that it is possible to cross the cyanine limit in the opposite direction (II → I) starting from a dissymmetric dipolar polymethine and increasing the solvent polarity.[22−24]

In the present contribution, we experimentally illustrate the existence of a third electronic configuration of polymethine dyes, corresponding to a predominant charge-centered state called bis-dipole[25] (form III, Figure 1). This electronic configuration is reminiscent of that of V-shaped chromophores;[26,27] it remains $C_{2v}$-symmetric but exhibits positive BLA and is associated with a broad charge transfer transition. Using a combined theory−experiment approach on cationic heptamethine dyes, we show that it is possible to tune the ground state configuration from cyanine to bis-dipole (I ⇆ III) by rational variation of the nature of the central substituent Y. To that end, a series of cationic heptamethines **1**−**10** (Figure 1) has been prepared with a wide range of Y substituents, namely, Cl, Br, SPh, OPh, OAc, H and various secondary, tertiary, and aromatic amino, alongside neutral heptamethines **11**−**14** featuring keto, malonitrile, and imino functionalities. Their absorption spectra are spread over the whole visible−NIR range, illustrating the dramatic influence of the Y substituent on the ground state electronic configuration. These data were compared to three independent parameters representative for the charge (de)localization: (i) the $^{13}C$ NMR chemical shift, (ii) the density functional theory (DFT) calculated BLA, and (iii) the calculated charge at the central position (C$\alpha$) of the bridge.

## RESULTS

**Synthesis.** The substitution of heptamethines at the central position has been widely studied.[28] The present homogeneous series of 17 polymethines reproduced already existing substitutions using synthetic protocols inspired by the literature but also described original substitutions like for compounds **2**, **7a,b,d**, **11**, **13**, and **14**. Experimental details and complete characterization of all chromophores are given in the Experimental Section and in Supporting Information. The synthesis of all derivatives used chloro- (respectively bromo-) heptamethine **1** (respectively **2**) as starting material (Figure 2), which were prepared by a Knoevenagel reaction between a chloro (respectively bromo) bis-aldehyde and an indolenium salt in basic, anhydrous conditions.[29] Heptamethines **3** and **5** were obtained under mild conditions as characteristic green powders with metallic shine by reacting **1** with thiophenol or phenol in the presence of cesium carbonate.[30−32] Alkylamino-substituted heptamethines **8**, **9**, and **10** were synthesized as glossy blue solids by heating **1** in the presence of the corresponding amine ($Et_2NH$, piperidine, *n*-$PrNH_2$) in DMF according to the procedure reported by Peng et al.[33] Aniline substituted derivatives **7a**−**d** were synthesized using a similar procedure.[34] It is worth noting that **7a,b** incorporating electron-deficient substituents required the use of microwave heating in a sealed tube to achieve the nucleophilic substitution in moderate yields. Heptamethine **6** was obtained by an original reductive debromination of **2** in the presence of sodium ethanethiolate in ethanethiol. The keto derivative **12** was synthesized according to the procedure described by Strekowski and co-workers[35] and was further used as precursor for the preparation of the ester derivative **4** by addition of acyl chloride at 0 °C.[6] Compound **11**, bearing dicyanovinyl fragment, was readily obtained by reaction of **1** with malononitrile in DMF.[36] Finally, in situ deprotonation of secondary amine based heptamethines **7c** and **10** by treatment with 1 M aqueous NaOH or $K_2CO_3$ solution led to the formation of neutral imine-substituted dyes **13** and **14**, respectively. All chromophores were characterized by HRMS and $^1H$ and $^{13}C$ NMR spectroscopy. $^1H$ NMR analyses unambiguously established that all compounds, regardless of the central substituent, are symmetric and present an all-trans configuration ($^3J_{trans} \approx 12-14$ Hz).

**Absorption Properties.** All compounds were studied by absorption spectroscopy in diluted dichloromethane or methanol solutions (Figure 3 and Table 1). Interestingly, in spite of strong structural similarities, chromophores **1**−**14** exhibit very different absorption spectra, whose maxima are spread over the 400−800 nm range. This feature highlights the dramatic influence of the central substitution on the electronic structure of these molecules. At first glance, two main behaviors can be distinguished: (i) heptamethines **1**−**6** with intense, sharp, and nonsolvatochromic (Figure S1) cyanine-type electronic transitions, all localized in a narrow near-infrared region (750−820 nm); (ii) heptamethines **7**−**14** with less intense, broad transitions covering the whole visible range (400−750 nm), indicating a loss of cyanine character. This transition exhibits a positive solvatochromism as illustrated by **11** (Figure S1). In particular, neutral heptamethines **11**−**14**


dx.doi.org/10.1021/jp501358q | J. Phys. Chem. A 2014, 118, 4038−4047

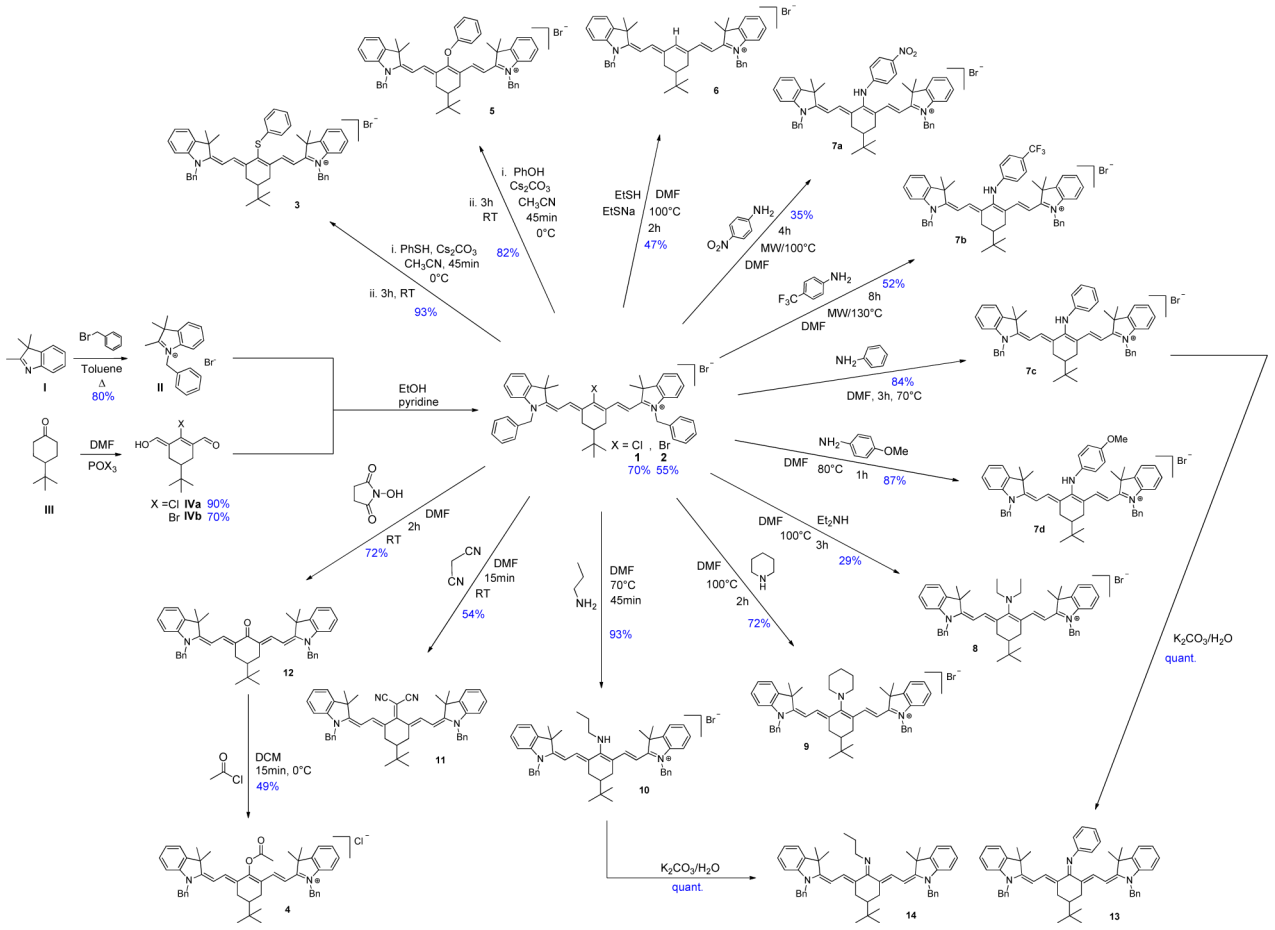

**Figure 2.** Synthetic scheme for compounds **1**−**14**.

with a central double bond undergo the strongest hypso- and hypochromic effects within the series. It can be noted that the absorption of aniline-substituted compound **7c** in dichloromethane (Figure 3, top) is located close to the frontier between the two above-mentioned tendencies. Fine modulation of the electronic density of aniline by introduction at the para position of electron-donating or -withdrawing moieties allows for exploring more specifically this region of interest. For solubility reason (Figure S2), the absorption spectra of heptamethines **7a**−**d** were recorded in diluted methanol solutions and compared to those of **1** and **10**, which are the hallmarks of the cyanine and non-cyanine behaviors, respectively. Whereas an electron-donating methoxy substituent on the aniline moiety (**7d**) induces a blue-shift of the absorption maximum, the opposite effect is observed for electron-withdrawing trifluoromethyl or nitro substituted derivatives **7a**,**b**. In addition, along this series, decreasing the electron density on the nitrogen atom induces a progressive hyperchromic effect accompanied by a sharpening of the transition as illustrated by the strong decrease of full width at half-maximum $\omega_{1/2}$ from 2521 to 925 $cm^{-1}$ for **7d** and **7a**, respectively (Table S2), bridging the gap between **10** and **1** ($\omega_{1/2}$ of 2688 and 768 $cm^{-1}$, respectively). In striking contrast with **7b**−**d**, **7a**, featuring the strongest electron-withdrawing nitro group, presents an absorption profile with an additional shoulder at higher energy, which corroborates the cyanine character of the associated electronic transition.

To rationalize the influence of the central substitution, we propose the following model: increasing the electron-donating ability of the central substituent Y progressively localizes the cationic charge on the central carbon atom of the polymethine chain. As a result, the delocalization of the charge on the $\pi$-conjugated skeleton is reduced and the cyanine character is lost. Instead, a bis-dipole electronic state is reached, which can be described as a central cationic acceptor bearing two electron-donating extremities (Figure 4). Within this model, polymethines **1**−**6** show a clear cyanine character, while dyes **7c**−**14** fall into the bis-dipole category.

At the frontier, intermediate behaviors are observed for **7a** and to a less extent **7b**, which correspond to the so-called cyanine limit. At the other extremity, neutral polymethines **11**−**14** can be depicted under their limit form where an anionic substituent faces a central highly localized carbocation (Figure 4). This model is in line with the explanation proposed by Marder and co-workers in the particular case of a dimethylamine-substituted polymethine.[37]

**Theoretical Calculations.** In a first approach, time-dependent density functional theory (TD-DFT) calculations were performed on the ground state optimized geometries of compounds **1** and **12** representatives for the cyanine and bis-dipole electronic configuration, respectively (see Experimental Section for computational details). The purpose was to identify the nature of the transitions involved in the cyanine and bis-dipole behaviors and to verify that those were in agreement with our model.

In the past, the intriguing optical properties of cyanine dyes have excited theoretical chemists who applied more or less sophisticated methodologies to deal with the computation of BLA, electronic excitation energies, or second- and third-order


dx.doi.org/10.1021/jp501358q | J. Phys. Chem. A 2014, 118, 4038−4047

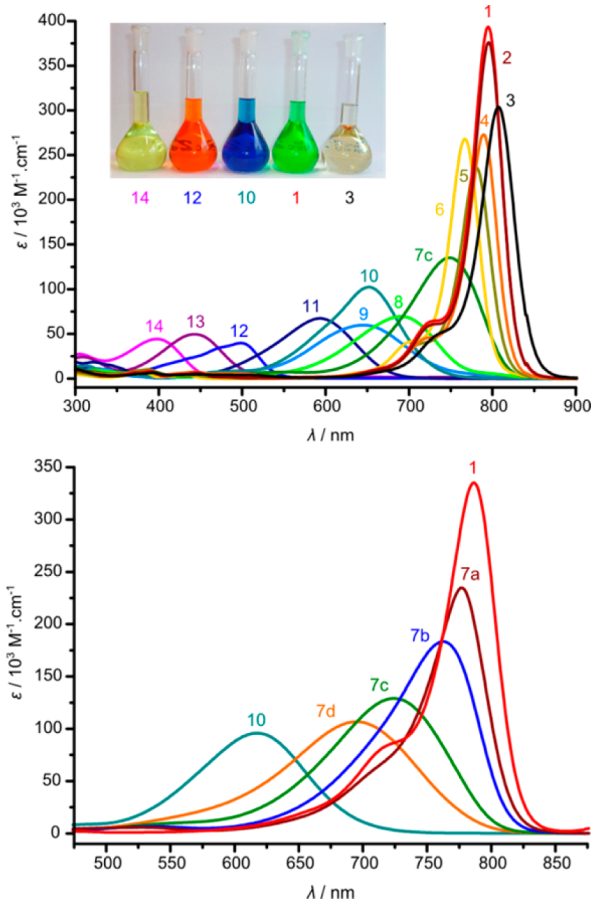


**Figure 3.** Absorption spectra of heptamethine dyes **1**–**6**, **7c**, **8**–**14** in dichloromethane at room temperature (top). Absorption spectra of aniline derivatives **7a**–**d** featuring $-NO_2$ (a), $-CF_3$ (b), $-H$ (c), and $-OMe$ (d) substituents in methanol at room temperature. Spectra of **1** and **10** in methanol were added for comparison (bottom).

polarizability.[38−43] In particular, numerous works were devoted to the question of the nonpertinence of TD-DFT for a correct description of electronic excitations energies in cyanine dyes.[44,45] As expected, vertical TD-DFT calculations do not properly reproduce the experimental $\lambda_{max}$ of the cyanine class,[46] whereas they are in excellent agreement in the case of **12** featuring a strong bis-dipole character (Table S3). In Figure 5, the density difference plots for these two compounds illustrate, on the one hand, the cyanine character of **1** with alternating regions of gain/loss of electron density presenting similar spatial extends. On the other hand, the bis-dipole nature of **12** is confirmed with red electron accepting zones (respectively blue electron donating regions) mainly localized at the center (respectively extremities) of the dye, though the usual red/blue alternating pattern, typical of transitions involving $\pi$ electrons, pertains. In order to gain further insights on the origin of the evolution of the band shapes, we determined vibronic spectra for **1** and **12** (Figure 5). First, we underline that the qualitative match with experimental absorption profiles of Figure 3 is remarkable, with **12** presenting a less intense and broader absorption profile located at higher energies. In comparison, the absolute transition energies of **1** are not very accurate, a known problem with TD-DFT (see above). Second, these simulations allowed identifying the vibrational modes responsible for the broadened shape of **12** and the hallmark shape of **1**. For the latter, the band asymmetry is explained by a series of

**Table 1. Absorption Maximum, $^{13}C$ NMR Chemical Shifts, Theoretical Bond Length Alternation, and Central Charges Determined for Heptamethines 1−14[a]**

| compd | $\lambda_{abs}$, nm | $\varepsilon$, $10^3$ $M^{-1}\cdot cm^{-1}$ | $^{13}C$ $\delta$, ppm | BLA, Å (M06-2X) | charge, $e$ (M06-2X) |
|---|---|---|---|---|---|
| **1** | 795 | 393 | 172.4 | 0.003 | 4.37 |
| | 786[b] | 335[b] | 174.4[b] | | |
| **2** | 795 | 376 | 172.6 | 0.001 | 4.35 |
| **3** | 807 | 304 | 172.4 | 0.004 | 3.86 |
| **4** | 789 | 273 | 172.0 | 0.002 | 4.36 |
| **5** | 780 | 236 | 172.1 | 0.002 | 4.29 |
| **6** | 767 | 268 | 171.5 | 0.002 | 3.77 |
| | 754[b] | 234[b] | 172.9[b] | | |
| **7a** | 777[b] | 235[b] | 172.9[b] | 0.004 | 4.20 |
| **7b** | 763[b] | 183[b] | 173.5[b] | 0.011 | 4.10 |
| **7c** | 748 | 135 | 172.9[b] | 0.016 | 3.92 |
| | 724[b] | 129[b] | | | |
| **7d** | 695[b] | 107[b] | 171.8[b] | 0.020 | 3.82 |
| **8** | 690 | 70 | 169.1 | 0.021 | 3.63 |
| | 685[b] | 79[b] | 170.7[b] | | |
| **9** | 646 | 60 | 167.2 | 0.024 | 3.46 |
| **10** | 652 | 102 | 166.0 | 0.027 | 3.36 |
| | 627[b] | 96[b] | 168.8[b] | | |
| **11** | 593 | 67 | 163.8 | 0.037 | 2.80 |
| **12** | 499 | 40 | 162.0 | 0.065 | 2.33 |
| **13** | 442[c] | 50[c] | 158.2[c] | 0.072 | 1.93 |
| **14** | 398[c] | 44[c] | 156.5[c] | 0.083 | 1.23 |

[a]Unless stated otherwise, all data were measured/calculated using $CH_2Cl_2$ as solvent ($CDCl_3$ for NMR data). [b]Measured in MeOH ($CD_3OD$ for NMR data). [c]Measured in situ by treatment with 1 M aqueous $K_2CO_3$ or NaOH solution.

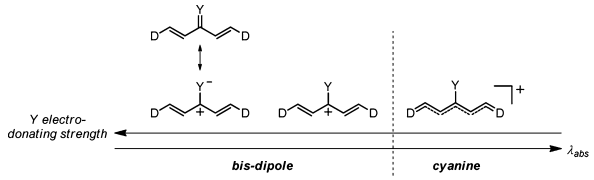


**Figure 4.** Electronic structure model showing the stabilization of the cationic charge at the central position as Y electron-donating strength increases.

low-frequency deformations, the 178th mode (1730 $cm^{-1}$) that corresponds to an asymmetric change of the character of the bonds in the conjugated pathway. In **12**, the 135th (1383 $cm^{-1}$) and 172th (1568 $cm^{-1}$) vibrational modes, mainly responsible for the emergence of the second peak, imply symmetric change of the single/double character of the bonds. Obviously such modes are more important when the BLA significantly departs from zero, which is consistent with their key role in **12** and their absence in **1**.

## DISCUSSION

To further validate our model, we investigated three additional parameters related to the charge (de)localization: (i) the experimental $^{13}C$ NMR chemical shift that is correlated to the electron density on an atom, (ii) the BLA, a well-known structural measure of the electronic delocalization, obtained on DFT optimized structures, and (iii) the calculated charge at the central position ($C_\alpha$) of the bridge.

We screened the charge density by measuring the $^{13}C$ chemical shift ($\delta$) of the $C_\omega$ carbon at the extremity of the


dx.doi.org/10.1021/jp501358q | J. Phys. Chem. A 2014, 118, 4038−4047

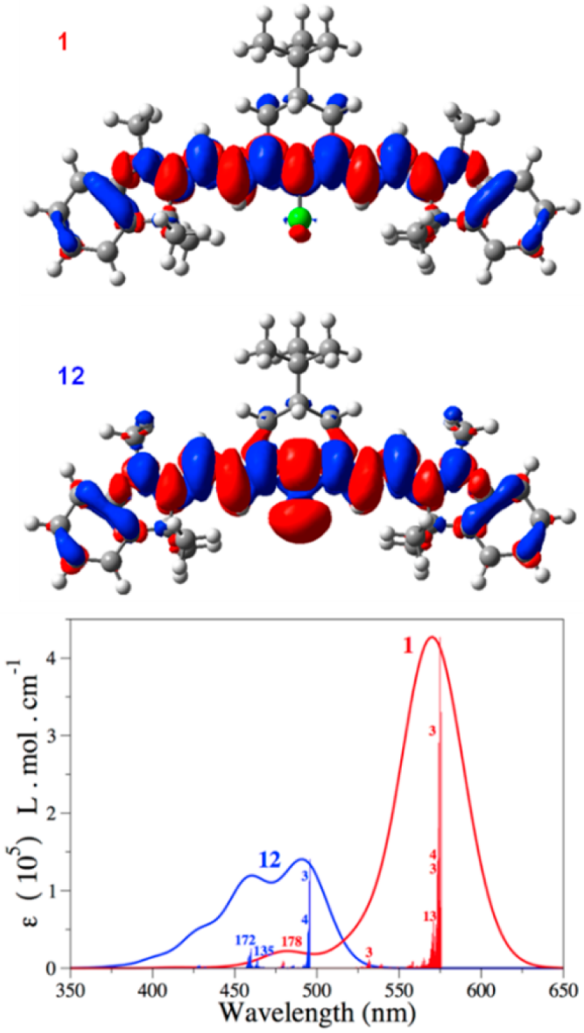


**Figure 5.** Density difference plots for the first excited state of **1** and **12** (top). The red (blue) zones indicate increase (decrease) of density upon electronic transition. Simulated vibrationally resolved spectra of **1** and **12** (bottom). For each system, the excited-state vibrational modes that strongly contribute to the band shape are displayed.

heptamethine bridge (Table 1, Figures 6).[47] According to our model, the progressive localization of the positive charge at the central $C_\alpha$ carbon toward a bis-dipole electronic structure should result in a higher electron density on the indolenine donor extremities of the molecule and consequently a larger shielding of the $C_\omega$ NMR signal. Experimentally, a 172 ± 0.5 ppm chemical shift is recorded for all dyes **1**−**6** exhibiting a cyanine-like absorption, signature of a perfect delocalization of the charge. As predicted, when the electron-donating strength of the central substituent increases, the signal is progressively shielded from 171 ppm for dye **7c** to ∼157 ppm for imine **14**.

This experimental observation is in agreement with the evolution of the APT charge (see Computational Details) borne by the central $C_\alpha$ carbon atom calculated at the PCM(DCM)-M06-2X/6-311G(2d,p) level (Table 1). Similar results are obtained with both PBE0 and ωB97X-D functionals or with MeOH as solvent (Tables S4−S6 and Figures S3 and S4). Once again, cyanine type compounds **1**−**6** present similar central charges with an average value of 4.17*e*. The aniline derivative **7c**, with a charge of 3.92*e*, exhibits an intermediate value between the cyanine and bis-dipole forms, while the bis-dipole dyes **8**−**14** cover a wide range of values, with decreasing charge from 3.36*e* for the amine derivative **10** to 1.23*e* for the corresponding imine **14**. These data are consistent with our model, since they indicate a progressive localization of the cationic charge at the center, thereby decreasing the electron density at $C_\alpha$ position. Finally, the BLA calculated on the optimized geometries allows discriminating between cyanine (BLA ≈ 0) and bis-dipole (BLA > 0) electronic structures (Table 1). As expected, **1**−**6** show a BLA very close to zero, whereas it progressively increases from **7** to **14** as the double bonds localize at the $C_\beta$−$C_\gamma$ and $C_\delta$−$C_\omega$ positions.

The validity of our model is further confirmed by the remarkable linear correlations that exist between the selected parameters representative for the degree of charge (de)-localization ($\delta(^{13}C)$, BLA, charge) and the lowest transition energy (Figure 7). In each case, heptamethines **1**−**6** featuring cyanine characters are bundled together in a narrow region, indicating almost identical electronic structure within this family. On the other hand, strong variations are observed among the bis-dipole family, illustrating very important electronic redistribution upon increasing electron-donating strength of the central substituent. The choice of the Y substituent is thus crucial to control the electronic structure of the polymethines. It is particularly striking that, in addition to the coarse tuning, fine-tuning can be also achieved as illustrated by the aniline series **7a**−**d**, where subtle variations of the electronic density on the nitrogen atom allow progressive movement from a bis-dipolar to a cyanine form.

## CONCLUSION

This study demonstrates the possibility of localizing the cationic charge at the central position of polymethine dyes owing to a rational tuning of the electron-donating ability of the central substituent. The ground-state electronic configuration resulting in this charge localization can be described as a bis-dipole, since it presents a charge transfer type transition from the lateral donor groups to the central carbocation, that is blue-shifted compared to that of related cyanine. It is possible to tune in both coarse and fine ways the magnitude of this hypsochromic shift by changing the electron-donating strength of the central substituent. This model was validated both experimentally and theoretically, and linear correlations were established between the evolution of the absorption spectra and the parameters relevant for the progressive charge (de)-localization over the conjugated backbone ($^{13}C$ NMR chemical shift, BLA extracted from DFT optimized geometries, and calculated APT charge).

On a broader perspective, this article proposes a more complete description of the spectral richness of polymethine dyes, nowadays ubiquitous in biology and materials science. It constitutes a strong evidence that this class of compounds should be depicted not only under two but also under three different ground state electronic configurations depending on the delocalized/localized character of the cationic charge: the cyanine with a fully delocalized charge, the dipole with a localized charge at one extremity, and now the bis-dipole with the charge localized at the central position. It is possible to favor one of the configurations by playing with the substitution of the polymethine or by exogenous parameters (solvent, temperature, counterion), and we believe that in the future the photophysical properties of the polymethine dyes should be rationalized using these three different configurations.


dx.doi.org/10.1021/jp501358q | J. Phys. Chem. A 2014, 118, 4038−4047

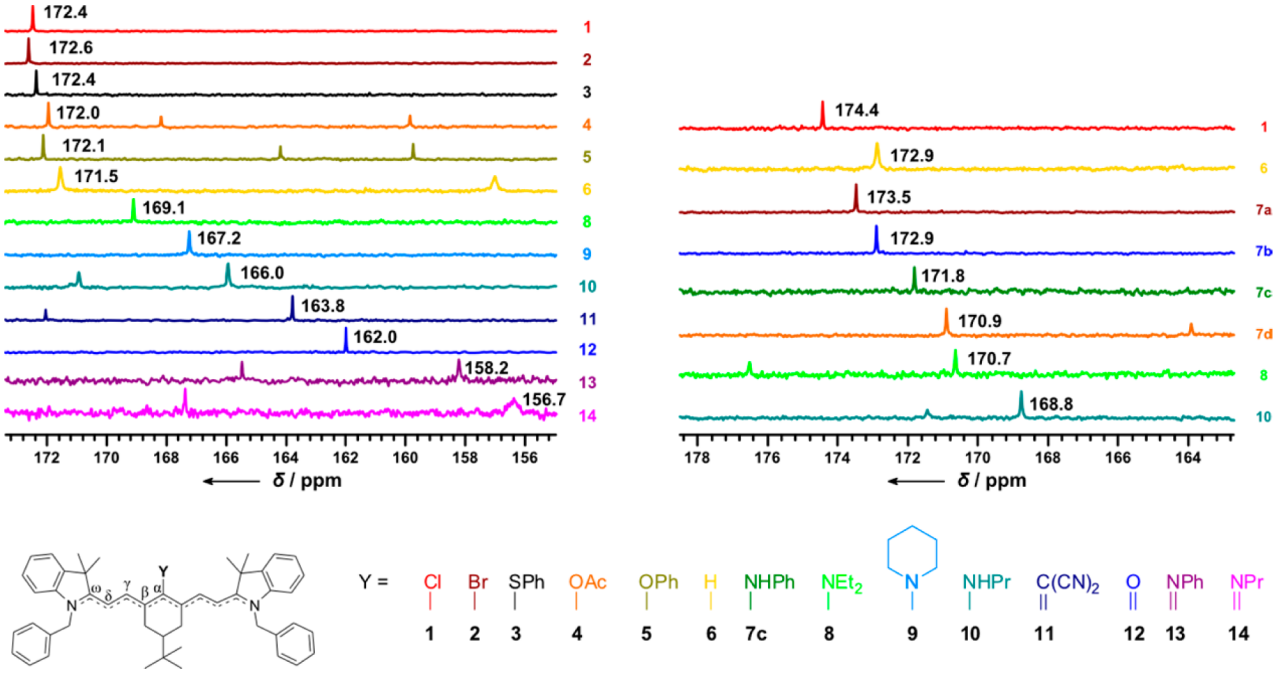


**Figure 6.** Comparison of $^{13}C$ NMR spectra in $CDCl_3$ (left) and $CD_3OD$ (right). Indicated chemical shifts are given for $C_\omega$ carbon atom.

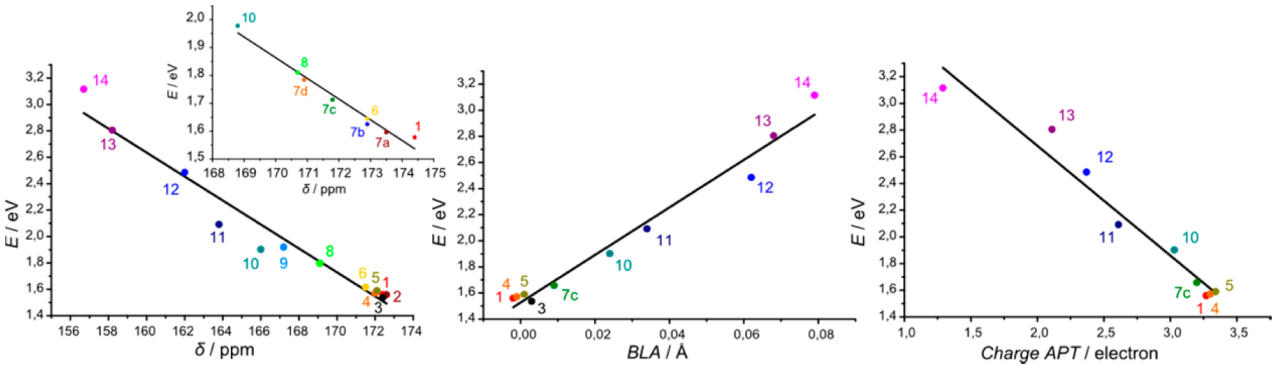


**Figure 7.** Correlation graphs plotting $\delta$ vs energy deduced from absorption in DCM (left), BLA vs energy (middle), and C$\alpha$ charge vs energy (right) and $\delta$ vs energy deduced from absorption in MeOH (inset).

## EXPERIMENTAL SECTION

**Computational Details.** All calculations were carried out with the Gaussian 09 program[48] tightening both self-consistent field ($10^{-10}$ au) and geometry optimization ($10^{-5}$ au) convergence thresholds. The calculations were performed on a structure in which the two side benzyl groups were replaced by methyl in order to lighten the computational burden. We have applied the default DFT integration grid, namely, a pruned (75 302) grid, except when convergence problem appeared and a tighter pruned (99 590) grid was necessary. For a given heptamethine, the same integration grid was systematically used for all steps of the computational protocol that consists of three successive stages: (1) the ground-state geometrical parameters were calculated at the DFT level, through a force-minimization process; (2) the vibrational spectrum of each derivative was determined analytically at the same level of theory, and it was checked that all structures correspond to true minima of the potential energy surface; (3) the first five low-lying excited states were calculated within the vertical linear-response TD-DFT approximation.[49,50] All atoms were described with the split-valence doubly polarized 6-311G(2d,p) atomic basis set. The solvent effects were accounted for with the polarizable continuum model (PCM),[51] with dichloromethane and methanol as selected solvents. Three functionals, namely, M06-2X,[52] PBE0,[53,54] and $\omega$B97X-D,[55] were considered. Atomic polar tensor (APT) charges, i.e., charges derived from the tensor of the derivatives of dipole moment with respect to atomic Cartesian coordinates,[56] were computed during the vibrational frequency calculations. Density difference plots corresponding to the relevant excited state were computed at the same levels of theory and are represented using a contour threshold of 0.0004 au. In these representations, blue (red) regions indicate loss (gain) of electron density upon transition.

Vibronic spectra were computed on the same structures (but for the replacement of the *t*-Bu group by a methyl) using a PCM-M06-2X/6-31G(d) protocol that has been shown to lead to reliable transition energies and band topologies.[57,58] The vibrationally resolved spectra (within the harmonic approximation) were computed using the FCclasses program.[59,60] The reported spectra were simulated using convoluting Gaussian functions presenting a full width at half-maximum (fwhm) of 0.08 eV. A maximal number of 25 overtones for each mode and


dx.doi.org/10.1021/jp501358q | J. Phys. Chem. A 2014, 118, 4038−4047

20 combination bands on each pair of modes were included in the calculation. The maximum number of integrals to be computed for each class was set to $1 \times 10^8$ or $1 \times 10^{10}$, and it was checked that such a number provides converged FC factors (>0.9).

**Synthesis. General Methods.** NMR spectra ($^1$H, $^{13}$C) were recorded at room temperature on a Bruker Advance instrument operating at 500.10 and 125.75 MHz for $^1$H and $^{13}$C, respectively. $^{13}$C NMR spectra were recorded using the $\mu$DEFT experiment,[61] and signals were assigned using HSQC and HMBC experiments. Data are listed in parts per million (ppm) and are reported relative to residual solvent peaks being used as internal standard ($^1$H ($CDCl_3$), 7.26 ppm; $^{13}$C ($CDCl_3$), 77.2 ppm; $^1$H ($CD_3OD$), 3.31 ppm; $^{13}$C ($CD_3OD$), 49.0 ppm). UV−visible spectra were recorded on a Jasco V-670 spectrophotometer in spectrophotometric grade methanol or dichloromethane solutions (about $10^{-5}$ or $10^{-6}$ mol $L^{-1}$). Molar extinction coefficients ($\varepsilon$) were determined at least two times. High resolution mass spectrometry measurements were performed at Centre Commun de Spectrometrie de Masse (Villeurbanne, France). Starting materials were purchased from Sigma-Aldrich, Acros Organics, or Alfa Aesar with the best available quality grade. All reactions were routinely performed under argon atmosphere in anhydrous solvents. Column chromatography was performed with Acros Organics (0.035−0.070 mm) silica gel. All reagents were purchased from commercial sources and used without further purification unless otherwise noted. Syntheses of precursors and of compounds **1**, **3**, **5**, **8**, **9**, **10** directly adapted from literature procedures are reported in Supporting Information.

**2.** To a solution of 100 mg of 5-*tert*-butyl-2-bromo-3-hydroxymethylenecyclohex-1-enecarbaldehyde (0.37 mmol, 1 equiv) and 277 mg of indolium salt (0.81 mmol, 2.2 equiv) in 8 mL of absolute ethanol was added 0.07 mL of pyridine (0.92 mmol, 2.5 equiv). The solution was stirred for 18 h at 40 °C. The resulting green solution was concentrated, dissolved in DCM, washed with an aqueous solution of HBr 1 M and an aqueous saturated $NaHCO_3$ solution. The organic layer was dried over $Na_2SO_4$, filtered, and concentrated. The crude was purified by flash chromatography on silica with DCM/methanol as eluent (98:2, $R_f$ = 0.18) and finally precipitated in $Et_2O$ to afford cyanine **2** as a green solid in a 55% yield (165 mg). $^1$H NMR ($CDCl_3$, 500.10 MHz): $\delta$ 8.25 (d, $^3J$ = 14 Hz, 2H), 7.43−7.24 (m, 18H), 6.22 (d, $^3J$ = 14 Hz, 2H), 5.54 (d, $^2J$ = 16.5 Hz, 2H), 5.45 (d, $^2J$ = 16.5 Hz, 2H), 2.64 (d, $^2J$ = 15 Hz, 2H), 2.09 (dd, $^2J$ = 14 Hz, $^3J$ = 13 Hz, 2H), 1.77 (s, 6H), 1.75 (s, 6H), 1.39 (m, 1H), 0.99 (s, 9H). $^{13}$C NMR ($CDCl_3$, 125.75 MHz): $\delta$ 172.6, 147.5, 146.7, 143.0, 141.1, 134.6, 130.7, 129.4, 129.1, 128.4, 126.8, 125.6, 122.5, 111.3, 103.1, 49.5, 48.7, 42.3, 32.5, 28.7, 28.3, 28.2, 27.6. UV−vis ($CH_3OH$) $\lambda_{max}$ = 787 nm ($\varepsilon_{max}$ = 297 000 L·mol$^{-1}$·cm$^{-1}$). UV−vis (DCM) $\lambda_{max}$ = 795 nm ($\varepsilon_{max}$ = 376 000 L·mol$^{-1}$·cm$^{-1}$). HRMS (ESI+): $[M]^+$ = 735.3325 (calcd for $C_{48}H_{52}BrN_2$, 735.3308).

**4.** To a solution of 65 mg of ketocyanine **12** (0.10 mmol, 1 equiv) in 5 mL of anhydrous DCM was added dropwise 0.07 mL of acetyl chloride (0.96 mmol, 10 equiv) at 0 °C. The mixture was stirred for 15 min at this temperature, then allowed to warm to room temperature, and finally quenched with one drop of distilled DIEA. The crude mixture was washed with an aqueous saturated NaCl solution; the organic layer was dried over $Na_2SO_4$, filtered, and concentrated. Flash column chromatography on silica using DCM/MeOH as eluent (95:5, $R_f$ = 0.19) afforded compound **4** as a green solid in 49% yield (34 mg). $^1$H NMR ($CDCl_3$, 500.10 MHz): $\delta$ 7.59 (d, $^3J_{trans}$ = 14 Hz, 2H), 7.40−7.38 (m, 2H), 7.38−7.30 (m, 8H), 7.29−7.22 (m, 6H), 7.18−7.17 (m, 2H), 6.06 (d, $^3J_{trans}$ = 14 Hz, 2H), 5.37 (m, 4H), 2.57 (d, $^2J$ = 15 Hz, 2H), 2.39 (s, 3H), 2.01 (dd, $^2J$ = 14 Hz, $^3J$ = 14 Hz, 2H), 1.68 (s, 6H), 1.65 (s, 6H), 1.47 (m, 1H), 0.97 (s, 9H). $^{13}$C NMR ($CDCl_3$, 125.75 MHz): $\delta$ 171.9, 168.2, 159.8, 142.9, 140.7, 140.2, 134.4, 129.5, 129.2, 128.6, 126.8, 125.6, 123.7, 122.5, 111.2, 101.8, 49.3, 48.6, 42.2, 32.6, 28.5, 28.4, 27.6, 25.5, 20.8. UV−vis ($CH_3OH$) $\lambda_{max}$ = 780 nm ($\varepsilon_{max}$ = 257 000 L·mol$^{-1}$·cm$^{-1}$). UV−vis (DCM) $\lambda_{max}$ = 789 nm ($\varepsilon_{max}$ = 273 000 L·mol$^{-1}$·cm$^{-1}$). HRMS (ESI+): $[M]^+$ = 715.4253 (calcd for $C_{50}H_{55}N_2O_2$, 715.4258).

**6.** Samples of 50 mg of cyanine **2** (0.06 mmol, 1 equiv), 103 mg of sodium ethanethiolate (1.22 mmol, 20 equiv), and 0.10 mL of ethanethiol (1.35 mmol, 22 equiv) were dissolved in 2 mL of anhydrous DMF and stirred for 2 h at 100 °C. The reaction mixture was allowed to cool to room temperature. DCM was added, and the sample was washed with water and an aqueous solution of HBr 1M. The organic layer was dried over $Na_2SO_4$ and finally concentrated. The crude residue was purified by flash chromatography on silica DCM/MeOH (90/10, $R_f$ = 0.44) to afford **6** as a green solid in a 47% yield (21 mg). $^1$H NMR ($CDCl_3$, 500.10 MHz): $\delta$ 7.74 (d, $^3J$ = 13 Hz, 2H), 7.59 (s, 1H), 7.39−7.27 (m, 14H), 7.21 (t, $^3J$ = 7 Hz, 2H), 7.10 (d, $^3J$ = 7 Hz, 2H), 5.99 (d, $^3J$ = 13 Hz, 2H), 5.27 (m, 4H), 2.44 (d, $^2J$ = 14 Hz, 2H), 1.84 (dd, $^2J$ = 13 Hz, $^3J$ = 13 Hz, 2H), 1.78 (s, 6H), 1.76 (s, 6H), 1.36 (m, 1H), 0.95 (s, 9H). $^{13}$C NMR ($CDCl_3$, 125.75 MHz): $\delta$ 171.5, 157.1, 149.0, 142.9, 141.0, 134.5, 134.1, 129.4, 128.8, 128.4, 126.7, 125.0, 122.6, 110.4, 100.7, 49.3, 48.1, 43.0, 32.6, 28.3, 28.2, 27.6, 25.2. UV−vis ($CH_3OH$) $\lambda_{max}$ = 754 nm ($\varepsilon_{max}$ = 234 000 L·mol$^{-1}$·cm$^{-1}$). UV−vis (DCM) $\lambda_{max}$ = 767 nm ($\varepsilon_{max}$ = 268 000 L·mol$^{-1}$·cm$^{-1}$). HRMS (ESI+): $[M]^+$ = 657.4189 (calcd for $C_{48}H_{53}N_2$, 657.4203).

**7a.** A solution of 100 mg of cyanine **1** (129 $\mu$mol, 1 equiv) and 120 mg of 4-nitroaniline (903 $\mu$mol, 7 equiv) in 2 mL of anhydrous DMF was stirred for 8 h at 130 °C under microwave irradiation. The reaction mixture was allowed to cool to room temperature and was extracted with DCM. The resulting organic phase was washed three times with an aqueous HBr 1 M solution, dried over $Na_2SO_4$, and evaporated. The crude residue was purified by flash column chromatography on silica with DCM/MeOH (from 97:3 to 95:5) as eluent to afford **7a** as a dark blue solid (40 mg, 35%). $^1$H NMR ($CD_3OD$, 500.10 MHz): $\delta$ 8.11 (d, $^3J$ = 8 Hz, 2H), 7.94 (d, $^3J$ = 14 Hz, 2H), 7.42 (d, $^3J$ = 7 Hz, 2H), 7.36−7.21 (m, 16H), 6.84 (d, $^3J$ = 7 Hz, 2H), 6.11 (d, $^3J$ = 13 Hz, 2H), 5.36 (d, $^2J$ = 16 Hz, 2H), 5.31 (d, $^2J$ = 16 Hz, 2H), 2.66 (d, $^2J$ = 14 Hz, 2H), 1.97 (dd, $^2J$ = 13 Hz, $^3J$ = 13 Hz, 2H), 1.41 (s, 6H), 1.40 (s, 6H), 1.31 (m, 1H), 0.99 (s, 9H). $^{13}$C NMR ($CD_3OD$, 125.75 MHz): $\delta$ 173.5, 156.0, 154.7, 144.3, 144.0, 142.2, 140.6, 136.3, 130.3, 129.9, 129.2, 128.5, 127.7, 127.4, 126.2, 123.6, 115.0, 111.8, 102.1, 50.1, 48.4, 44.4, 33.4, 28.3, 28.3, 27.7, 26.9. UV−vis ($CH_3OH$) $\lambda_{max}$ = 777 nm ($\varepsilon_{max}$ = 235 000 L·mol$^{-1}$·cm$^{-1}$). HRMS (ESI+): $[M]^+$ = 793.4460 (calcd for $C_{54}H_{57}N_4O_2$, 793.4476).

**7b.** A solution of 100 mg of cyanine **1** (129 $\mu$mol, 1 equiv) and 81 $\mu$L of 4-trifluoromethylaniline (647 $\mu$mol, 5 equiv) in 2 mL of anhydrous DMF was stirred for 4 h at 100 °C under microwave irradiation. The reaction mixture was allowed to cool to room temperature and was extracteed with DCM. The resulting organic phase was washed twice with an aqueous HBr 1 M solution, dried over $Na_2SO_4$, and evaporated. The crude residue was purified by flash column chromatography on silica


dx.doi.org/10.1021/jp501358q | J. Phys. Chem. A 2014, 118, 4038−4047

with DCM/MeOH (from 97:3 to 95:5) as eluent to afford compound **7b** as a dark blue solid (60 mg, 52%). $^1$H NMR ($CD_3OD$, 500.10 MHz): $\delta$ 7.98 (d, $^3J$ = 14 Hz, 2H), 7.50 (d, $^3J$ = 8 Hz, 2H), 7.42 (d, $^3J$ = 7 Hz, 2H), 7.37−7.19 (m, 16H), 6.98 (d, $^3J$ = 8 Hz, 2H), 6.02 (d, $^3J$ = 14 Hz, 2H, 5.31 (s, 4H), 2.62 (d, $^2J$ = 15 Hz, 2H), 1.91 (dd, $^2J$ = 14 Hz, $^3J$ = 14 Hz, 2H), 1.40 (s, 6H), 1.39 (s, 6H), 1.29 (m, 1H), 0.97 (s, 9H). $^{13}$C NMR ($CD_3OD$, 125.75 MHz): $\delta$ 172.9, 158.8, 151.4, 144.4, 144.2, 142.0, 136.4, 130.2, 129.8, 129.3, 129.1, 128.2, 128.2, 127.6, 127.2, 125.8, 123.5, 117.0, 111.4, 101.1, 49.9, 48.4, 44.7, 33.4, 28.4, 28.4, 27.7, 26.9. UV−vis ($CH_3OH$) $\lambda_{max}$ = 763 nm ($\varepsilon_{max}$ = 183 000 L·mol$^{-1}$·cm$^{-1}$). HRMS (ESI+): $[M]^+$ = 816.4474 (calcd for $C_{55}H_{57}F_3N_3$, 816.4499).

**7c.** A solution of 200 mg of cyanine **1** (0.26 mmol, 1 equiv) and 94 $\mu$L of distilled aniline (1.04 mmol, 4 equiv) in 3 mL of anhydrous DMF was stirred for 8h at 70 °C. The reaction mixture was allowed to cool to room temperature and was extracted with DCM. The resulting organic phase was washed three times with an aqueous HBr 1 M solution, dried over $Na_2SO_4$, and concentrated. The crude residue was purified by flash chromatography on silica with EtOAc/DCM/MeOH (from 50:50:0 to 45:45:10) as eluent to afford **7c** as a dark blue solid in 84% yield (180 mg). $^1$H NMR ($CD_3OD$, 500.10 MHz): $\delta$ 7.99 (d, $^3J$ = 14 Hz, 2H), 7.38 (d, $^3J$ = 7 Hz, 2H), 7.34−7.27 (m, 9H), 7.24−7.14 (m, 9H), 7.03 (d, $^3J$ = 8 Hz, 2H), 6.87 (t, $^3J$ = 7 Hz, 1H), 5.89 (d, $^3J$ = 14 Hz, 2H), 5.26 (d, $^2J$ = 17 Hz, 2H), 5.22 (d, $^2J$ = 17 Hz, 2H), 2.57 (dd, $^2J$ = 12 Hz, $^3J$ = 3 Hz, 2H), 1.82 (dd, $^2J$ = 13 Hz, $^3J$ = 13 Hz, 2H), 1.40 (s, 6H), 1.38 (s, 6H), 1.33 (m, 1H), 0.92 (s, 9H). $^{13}$C NMR ($CD_3OD$, 125.75 MHz): $\delta$ 171.8, 162.3, 147.2, 144.6, 143.9, 141.8, 136.5, 131.1, 130.2, 129.9, 129.7, 129.0, 127.6, 125.2, 123.4, 122.9, 119.6, 110.9, 99.7, 49.6, 48.2, 45.1, 33.4, 28.6, 28.6, 27.6, 27.0. UV−vis ($CH_3OH$) $\lambda_{max}$ = 724 nm ($\varepsilon_{max}$ = 129 000 L·mol$^{-1}$·cm$^{-1}$). HRMS (ESI+): $[M]^+$ = 748.4625 (calcd for $C_{54}H_{58}N_3$, 748.4625).

**7d.** A solution of 100 mg of cyanine **1** (0.13 mmol, 1 equiv) and 64 mg of *p*-anisidine (0.52 mmol, 4 equiv) in 2 mL of anhydrous DMF was stirred for 1 h at 80 °C. The reaction mixture was allowed to cool to room temperature, and DMF was evaporated. Then DCM was added and the organic layer was washed with an aqueous HBr 1 M solution and water, dried over $Na_2SO_4$, and concentrated. The crude residue was purified by flash chromatography on silica with DCM/MeOH (95:5, $R_f$ = 0.56) as eluent and precipitated in pentane to afford compound **7d** as a dark blue solid in 87% yield (97 mg). $^1$H NMR ($CD_3OD$, 500.10 MHz): $\delta$ 7.93 (d, $^3J$ = 13 Hz, 2H), 7.36−7.06 (m, 20H), 6.90 (d, $^3J$ = 7 Hz, 2H), 5.79 (d, $^3J$ = 13 Hz, 2H), 5.22 (d, $^2J$ = 17 Hz, 2H), 5.16 (d, $^2J$ = 17 Hz, 2H), 3.74 (s, 3H), 2.51 (d, $^2J$ = 13 Hz, 2H), 1.76 (dd, $^2J$ = 13 Hz, $^3J$ = 13 Hz, 2H), 1.41 (s, 6H), 1.38 (s, 6H), 1.26 (m, 1H), 0.87 (s, 9H). $^{13}$C NMR ($CD_3OD$, 125.75 MHz): $\delta$ 170.9, 163.9, 157.2, 144.8, 143.1, 141.5, 139.7, 136.6, 130.2, 129.6, 128.9, 127.5, 124.9, 123.3, 122.5, 116.6, 110.6, 98.7, 56.1, 48.8, 48.0, 45.3, 33.4, 28.7, 28.6, 27.6, 27.1 (1 $C_{quat}$ is missing). UV−vis ($CH_3OH$) $\lambda_{max}$ = 695 nm ($\varepsilon_{max}$ = 107 000 L·mol$^{-1}$·cm$^{-1}$). HRMS (ESI+): $[M]^+$ = 778.4714 (calcd for $C_{55}H_{60}N_3O$, 778.4731).

**11.** To a solution of 30 mg of cyanine **1** (0.04 mmol, 1 equiv) and 3.8 mg of malononitrile (0.06 mmol, 1.5 equiv) in 2 mL of anhydrous DMF was added 0.01 mL of distilled DIEA (0.08 mmol, 2 equiv), and the mixture was stirred for 15 min at room temperature. Then DCM was added to the solution. The organic layer was washed with an aqueous saturated solution of $NH_4Cl$, dried over $Na_2SO_4$, and concentrated. A purification by flash column chromatography on silica with DCM/MeOH (98:2, $R_f$ = 0.83) affords compound **11** as a blue solid in a 54% yield (15 mg). $^1$H NMR ($CDCl_3$, 500.10 MHz): $\delta$ 7.63 (d, $^3J_{trans}$ = 13 Hz, 2H), 7.33−7.26 (m, 6H), 7.23−7.20 (m, 4H), 7.00 (t, $^3J$ = 7 Hz, 2H), 6.81 (d, $^3J$ = 8 Hz, 2H), 5.46 (d, $^3J_{trans}$ = 13 Hz, 2H), 4.95 (d, $^2J$ = 17 Hz, 2H), 4.87 (d, $^2J$ = 17 Hz, 2H), 2.33 (dd, $^2J$ = 15 Hz, $^3J$ = 4 Hz, 2H), 1.74 (s, 6H), 1.67 (s, 6H), 1.65 (m, 2H), 1.24 (m, 1H), 0.76 (s, 9H). $^{13}$C NMR ($CDCl_3$, 125.75 MHz): $\delta$ 172.0, 163.8, 144.3, 140.4, 135.8, 134.4, 129.2, 128.1, 127.8, 127.3, 126.5, 122.3, 121.7, 120.4, 107.5, 94.8, 57.7, 47.1, 46.9, 43.5, 32.7, 30.1, 29.5, 27.4, 27.2. UV−vis ($CH_3OH$) $\lambda_{max}$ = 630 nm ($\varepsilon_{max}$ = 75 600 L·mol$^{-1}$·cm$^{-1}$). UV−vis (DCM) $\lambda_{max}$ = 593 nm ($\varepsilon_{max}$ = 67 000 L·mol$^{-1}$·cm$^{-1}$). HRMS (ESI+): $[M + H]^+$ = 721.4241 (calcd for $C_{51}H_{53}N_4$, 721.4265).

**12.** To a solution of 40 mg of cyanine **1** (0.05 mmol, 1 equiv) and 12 mg of *N*-hydroxysuccinimide (0.10 mmol, 2 equiv) in 5 mL of anhydrous DMF was added 0.02 mL of distilled DIEA (0.10 mmol, 2 equiv), and the mixture was stirred for 2 h at room temperature. Then an amount of 10 mL of DCM was added to the solution. The organic layer was washed with an aqueous saturated solution of $NH_4Cl$ (10 mL) and water (10 mL), dried over $Na_2SO_4$, and concentrated. After filtration through an activated alumina plug (25 g of $Al_2O_3$ with 6% $H_2O$) with DCM/petroleum ether (1:1, $R_f$ = 0.26), compound **12** was isolated as a red solid in a 86% yield (30 mg). $^1$H NMR ($CDCl_3$, 500.10 MHz): $\delta$ 8.04 (d, $^3J$ = 13 Hz, 2H), 7.33−7.30 (m, 4H), 7.27−7.22 (m, 8H), 7.17 (t, $^3J$ = 8 Hz, 2H), 6.94 (t, $^3J$ = 7 Hz, 2H), 6.72 (d, $^3J$ = 8 Hz, 2H), 5.42 (d, $^3J$ = 13 Hz, 2H), 4.91 (d, $^2J$ = 16 Hz, 2H), 4.84 (d, $^2J$ = 16 Hz, 2H), 2.57 (dd, $^2J$ = 15 Hz, $^3J$ = 3 Hz, 2H), 1.88 (dd, $^2J$ = 14 Hz, $^3J$ = 14 Hz, 2H), 1.70 (s, 12H), 1.34 (m, 1H), 0.90 (s, 9H). $^{13}$C NMR ($CDCl_3$, 125.75 MHz): $\delta$ 186.7, 162.0, 144.8, 139.6, 136.4, 132.4, 129.0, 127.9, 127.6, 127.5, 126.7, 122.0, 120.8, 106.8, 94.0, 46.7, 46.6, 43.3, 32.6, 28.9, 28.9, 27.5, 26.7. UV−vis ($CH_3OH$) $\lambda_{max}$ = 526 nm ($\varepsilon_{max}$ = 50 000 L·mol$^{-1}$·cm$^{-1}$). UV−vis (DCM) $\lambda_{max}$ = 499 nm ($\varepsilon_{max}$ = 40 000 L·mol$^{-1}$·cm$^{-1}$). HRMS (ESI+): $[M + H]^+$ = 673.4120 (calcd for $C_{48}H_{53}N_2O$, 673.4152).

**13.** Compound **13** was quantitatively formed by treatment of a solution of compound **7c** in DCM or $CDCl_3$ with an aqueous $K_2CO_3$ solution (1 M). Analyses were performed in situ. $^1$H NMR ($CDCl_3$, 500.10 MHz): $\delta$ 7.28−7.19 (m, 18H), 6.87−6.80 (m, 5H), 6.62 (d, $^3J$ = 8 Hz, 2H), 5.23 (d, $^3J$ = 12 Hz, 2H), 4.77 (m, 4H), 2.45 (d, $^2J$ = 12 Hz, 2H), 1.83 (dd, $^2J$ = 14 Hz, $^3J$ = 14 Hz, 2H), 1.40−1.29 (m, 13H), 0.84 (s, 9H). $^{13}$C NMR ($CDCl_3$, 125.75 MHz): $\delta$ 165.5, 158.2, 154.4, 145.2, 139.3, 136.8, 133.6, 129.5, 128.9, 127.8, 127.4, 126.7, 121.9, 120.9, 120.1, 120.0, 106.1, 93.8, 46.5, 45.6, 43.7, 32.7, 28.7, 28.5, 27.8, 27.4 (1 CH is missing). UV−vis (DCM) $\lambda_{max}$ = 442 nm ($\varepsilon_{max}$ = 50 000 L·mol$^{-1}$·cm$^{-1}$).

**14**. Compound **14** was quantitatively formed by treatment of compound **10** in DCM or $CDCl_3$ with an aqueous $K_2CO_3$ solution (1 M). Analyses were performed in situ. $^1$H NMR ($CDCl_3$, 500.10 MHz): $\delta$ 7.29−7.21 (m, 12H), 7.17−7.11 (m, 4H), 6.84 (t, 2H, $^3J$ = 7 Hz), 6.63 (d, 2H, $^3J$ = 8 Hz), 5.25 (d, $^3J$ = 12 Hz, 2H), 4.78 (m, 4H), 3.56 (t, 2H, $^3J$ = 7 Hz), 2.41−2.38 (m, 2H), 1.82−1.78 (m, 2H), 1.70 (m, 2H), 1.62 (bs, 6H), 1.59 (bs, 6H), 1.31 (m, 1H), 1.02 (t, $^3J$ = 7 Hz, 3H), 0.81 (s, 9H). $^{13}$C NMR ($CDCl_3$, 125.75 MHz): $\delta$ 167.5, 156.5, 145.5, 139.1, 137.0, 128.9 (HSQC showed that two carbons have this $\delta$), 127.8, 127.4, 126.7, 121.9, 119.7, 106.0, 94.4, 55.5, 46.6, 45.5,


dx.doi.org/10.1021/jp501358q | J. Phys. Chem. A 2014, 118, 4038−4047

43.7, 32.6, 28.7, 27.4, 25.9, 12.3 (1 $C_{quat}$ is missing). UV−vis (DCM) $\lambda_{max}$ = 398 nm ($\varepsilon_{max}$ = 44 000 L·mol$^{-1}$·cm$^{-1}$).

## ■ ASSOCIATED CONTENT

### Supporting Information

Full width at half-maximum data extracted from absorption spectra, solvatochromism experiments, additional theoretical data, concentration-dependent absorption study, synthesis details, and complete characterizations including NMR spectra of all compounds. This material is available free of charge via the Internet at http://pubs.acs.org.

## ■ AUTHOR INFORMATION

### Corresponding Authors

*B.L.G.: e-mail, boris.leguennic@univ-rennes1.fr.
*C.A.: fax, (+)33472728860; e-mail, chantal.andraud@ens-lyon.fr.
*O.M.: fax, (+)33472728860; e-mail, olivier.maury@ens-lyon.fr.

### Notes

The authors declare no competing financial interest.

## ■ ACKNOWLEDGMENTS

A.C.-E. thanks the European Research Council (ERC, Marches 278845) for his postdoctoral grant. D.J. acknowledges the European Research Council (ERC) and the Région des Pays de la Loire for financial support in the framework of a starting grant (Marches 278845) and a recrutement sur poste stratégique, respectively. This research used resources of (1) the GENCI-CINES/IDRIS (Grant c2012085117), (2) CCIPL (Centre de Calcul Intensif des Pays de Loire), and (3) a local Troy cluster.

## ■ REFERENCES

(1) Fabian, J.; Nakazumi, H.; Matsuoka, M. Near-Infrared Absorbing Dyes. *Chem. Rev.* **1992**, *92*, 1197−1226.
(2) Mishra, A.; Behera, R. K.; Behera, P. K.; Mishra, B. K.; Behera, G. B. Cyanines During the 1990s: A Review. *Chem. Rev.* **2000**, *100*, 1973−2012.
(3) Frangioni, J. V. In Vivo Near-Infrared Fluorescence Imaging. *Curr. Opin. Chem. Biol.* **2003**, *7*, 626−634.
(4) Kiyose, K.; Kojima, H.; Nagano, T. Functional Near-Infrared Fluorescent Probes. *Chem.—Asian J.* **2008**, *3*, 506−515.
(5) Przhonska, O.; Webster, S.; Padilha, L.; Hu, H.; Kachkovski, A.; Hagan, D.; Stryland, E. Two-Photon Absorption in Near-IR Conjugated Molecules: Design Strategy and Structure−Property Relations. In *Advanced Fluorescence Reporters in Chemistry and Biology I*; Demchenko, A. P., Ed.; Springer: Berlin and Heidelberg, Germany, 2010; Vol. *8*, pp 105−147.
(6) Hu, C.; Sun, W.; Cao, J.; Gao, P.; Wang, J.; Fan, J.; Song, F.; Sun, S.; Peng, X. A Ratiometric Near-Infrared Fluorescent Probe for Hydrazine and Its in Vivo Applications. *Org. Lett.* **2013**, *15*, 4022−4025.
(7) Wang, X.; Sun, J.; Zhang, W.; Ma, X.; Lv, J.; Tang, B. A Near-Infrared Ratiometric Fluorescent Probe for Rapid and Highly Sensitive Imaging of Endogenous Hydrogen Sulfide in Living Cells. *Chem. Sci.* **2013**, *4*, 2551−2556.
(8) Hales, J. M.; Matichak, J.; Barlow, S.; Ohira, S.; Yesudas, K.; Brédas, J.-L.; Perry, J. W.; Marder, S. R. Design of Polymethine Dyes with Large Third-Order Optical Nonlinearities and Loss Figures of Merit. *Science* **2010**, *327*, 1485−1488.
(9) Bellier, Q.; Makarov, N. S.; Bouit, P.-A.; Rigaut, S.; Kamada, K.; Feneyrou, P.; Berginc, G.; Maury, O.; Perry, J. W.; Andraud, C. Excited State Absorption: A Key Phenomenon for the Improvement of Biphotonic Based Optical Limiting at Telecommunication Wavelengths. *Phys. Chem. Chem. Phys.* **2012**, *14*, 15299−15307.
(10) Bouit, P.-A.; Di Piazza, E.; Rigaut, S.; Le Guennic, B.; Aronica, C.; Toupet, L.; Andraud, C.; Maury, O. Stable Near-Infrared Anionic Polymethine Dyes: Structure, Photophysical, and Redox Properties. *Org. Lett.* **2008**, *10*, 4159−4162.
(11) Terenziani, F.; Painelli, A.; Katan, C.; Charlot, M.; Blanchard-Desce, M. Charge Instability in Quadrupolar Chromophores: Symmetry Breaking and Solvatochromism. *J. Am. Chem. Soc.* **2006**, *128*, 15742−15755.
(12) Terenziani, F.; Przhonska, O. V.; Webster, S.; Padilha, L. A.; Slominsky, Y. L.; Davydenko, I. G.; Gerasov, A. O.; Kovtun, Y. P.; Shandura, M. P.; Kachkovski, A. D.; Hagan, D. J.; Van Stryland, E. W.; Painelli, A. Essential-State Model for Polymethine Dyes: Symmetry Breaking and Optical Spectra. *J. Phys. Chem. Lett.* **2010**, *1*, 1800−1804.
(13) Dähne, S.; Radeglia, R. Revision der Lewis-Calvin-Regel zur Charakterisierung Vinyloger Polyen- und Polymethinähnlicher Verbindungen. *Tetrahedron* **1971**, *27*, 3673−3693.
(14) Dähne, S. Color and Constitution: One Hundred Years of Research. *Science* **1978**, *199*, 1163−1167.
(15) Marder, S. R.; Gorman, C. B.; Tiemann, B. G.; Perry, J. W.; Bourhill, G.; Mansour, K. Relation between Bond-Length Alternation and Second Electronic Hyperpolarizability of Conjugated Organic Molecules. *Science* **1993**, *261*, 186−189.
(16) Brooker, L. G. S.; Sprague, R. H.; Smyth, C. P.; Lewis, G. L. Color and Constitution. I. Halochromism of Anhydronium Bases Related to the Cyanine Dyes 1. *J. Am. Chem. Soc.* **1940**, *62*, 1116−1125.
(17) Tolbert, L. M.; Zhao, X. Beyond the Cyanine Limit: Peierls Distortion and Symmetry Collapse in a Polymethine Dye. *J. Am. Chem. Soc.* **1997**, *119*, 3253−3258.
(18) Lepkowicz, R. S.; Przhonska, O. V.; Hales, J. M.; Fu, J.; Hagan, D. J.; Van Stryland, E. W.; Bondar, M. V.; Slominsky, Y. L.; Kachkovski, A. D. Nature of the Electronic Transitions in Thiacarbocyanines with a Long Polymethine Chain. *Chem. Phys.* **2004**, *305*, 259−270.
(19) Hu, H.; Przhonska, O. V.; Terenziani, F.; Painelli, A.; Fishman, D.; Ensley, T. R.; Reichert, M.; Webster, S.; Bricks, J. L.; Kachkovski, A. D.; Hagan, D. J.; Van Stryland, E. W. Two-Photon Absorption Spectra of a Near-Infrared 2-Azaazulene Polymethine Dye: Solvation and Ground-State Symmetry Breaking. *Phys. Chem. Chem. Phys.* **2013**, *15*, 7666−7678.
(20) Bouit, P.-A.; Aronica, C.; Toupet, L.; Le Guennic, B.; Andraud, C.; Maury, O. Continuous Symmetry Breaking Induced by Ion Pairing Effect in Heptamethine Cyanine Dyes: Beyond the Cyanine Limit. *J. Am. Chem. Soc.* **2010**, *132*, 4328−4335.
(21) Pascal, S.; Bouit, P.-A.; Le Guennic, B.; Parola, S.; Maury, O.; Andraud, C. Symmetry Loss of Heptamethine Cyanines: An Example of Dipole Generation by Ion-Pairing Effect. *Proc. SPIE* **2013**, *8622* (86220F), 1−7.
(22) Würthner, F.; Archetti, G.; Schmidt, R.; Kuball, H.-G. Solvent Effect on Color, Band Shape, and Charge-Density Distribution for Merocyanine Dyes Close to the Cyanine Limit. *Angew. Chem., Int. Ed.* **2008**, *47*, 4529−4532.
(23) Rettig, W.; Dekhtyar, M. Merocyanines: Polyene−Polymethine Transition in Donor−Acceptor-Substituted Stilbenes and Polyenes. *Chem. Phys.* **2003**, *293*, 75−90.
(24) Mustroph, H.; Mistol, J.; Senns, B.; Keil, D.; Findeisen, M.; Hennig, L. Relationship between the Molecular Structure of Merocyanine Dyes and the Vibrational Fine Structure of Their Electronic Absorption Spectra. *Angew. Chem., Int. Ed.* **2009**, *48*, 8773−8775.
(25) Since the structures are formally noncentrosymmetric, the denomination quadrupole cannot be applied.
(26) Sissa, C.; Terenziani, F.; Painelli, A.; Siram, R. B. K.; Patil, S. Spectroscopic Characterization and Modeling of Quadrupolar Charge-Transfer Dyes with Bulky Substituents. *J. Phys. Chem. B* **2012**, *116*, 4959−4966.

(27) Zou, Q.; Zhao, Y.; Makarov, N. S.; Campo, J.; Yuan, H.; Fang, D.-C.; Perry, J. W.; Wu, F. Effect of Alicyclic Ring Size on the Photophysical and Photochemical Properties of Bis(arylidene)-cycloalkanone Compounds. *Phys. Chem. Chem. Phys.* **2012**, *14*, 11743−11752.
(28) Strekowski, L.; Lipowska, M.; Patonay, G. Substitution Reactions of a Nucleofugal Group in Heptamethine Cyanine Dyes. Synthesis of an Isothiocyanato Derivative for Labeling of Proteins with a Near-Infrared Chromophore. *J. Org. Chem.* **1992**, *57*, 4578−4580.
(29) Reynolds, G. A.; Drexhage, K. H. Stable Heptamethine Pyrylium Dyes That Absorb in the Infrared. *J. Org. Chem.* **1977**, *42*, 885−888.
(30) Gallaher, D. L., Jr.; Johnson, M. E. Development of Near-Infrared Fluorophoric Labels for the Determination of Fatty Acids Separated by Capillary Electrophoresis with Diode Laser Induced Fluorescence Detection. *Analyst* **1999**, *124*, 1541−1546.
(31) Flanagan, J. H.; Khan, S. H.; Menchen, S.; Soper, S. A.; Hammer, R. P. Functionalized Tricarbocyanine Dyes as Near-Infrared Fluorescent Probes for Biomolecules. *Bioconjugate Chem.* **1997**, *8*, 751−756.
(32) Bouit, P.-A.; Spänig, F.; Kuzmanich, G.; Krokos, E.; Oelsner, C.; Garcia-Garibay, M. A.; Delgado, J. L.; Martín, N.; Guldi, D. M. Efficient Utilization of Higher-Lying Excited States to Trigger Charge-Transfer Events. *Chem.—Eur. J.* **2010**, *16*, 9638−9645.
(33) Peng, X.; Song, F.; Lu, E.; Wang, Y.; Zhou, W.; Fan, J.; Gao, Y. Heptamethine Cyanine Dyes with a Large Stokes Shift and Strong Fluorescence: A Paradigm for Excited-State Intramolecular Charge Transfer. *J. Am. Chem. Soc.* **2005**, *127*, 4170−4171.
(34) Kiyose, K.; Aizawa, S.; Sasaki, E.; Kojima, H.; Hanaoka, K.; Terai, T.; Urano, Y.; Nagano, T. Molecular Design Strategies for Near-Infrared Ratiometric Fluorescent Probes Based on the Unique Spectral Properties of Aminocyanines. *Chem.—Eur. J.* **2009**, *15*, 9191−9200.
(35) Strekowski, L.; Mason, J. C.; Say, M.; Lee, H.; Gupta, R.; Hojjat, M. Novel Synthetic Route to pH-Sensitive 2,6-Bis(substituted ethylidene)cyclohexanone/hydroxycyanine Dyes That Absorb in the Visible/Near-Infrared Regions. *Heterocycl. Commun.* **2005**, *11*, 129−134.
(36) Mayerhöffer, U.; Gsänger, M.; Stolte, M.; Fimmel, B.; Würthner, F. Synthesis and Molecular Properties of Acceptor-Substituted Squaraine Dyes. *Chem.—Eur. J.* **2013**, *19*, 218−232.
(37) Matichak, J. D.; Hales, J. M.; Barlow, S.; Perry, J. W.; Marder, S. R. Dioxaborine- and Indole-Terminated Polymethines: Effects of Bridge Substitution on Absorption Spectra and Third-Order Polarizabilities. *J. Phys. Chem. A* **2011**, *115*, 2160−2168.
(38) Fabian, J. Symmetry-Lowering Distortion of Near-Infrared Polymethine Dyes—A Study by First-Principles Methods. *J. Mol. Struct.: THEOCHEM* **2006**, *766*, 49−60.
(39) Masunov, A.; Tretiak, S. Prediction of Two-Photon Absorption Properties for Organic Chromophores Using Time-Dependent Density-Functional Theory. *J. Phys. Chem. B* **2003**, *108*, 899−907.
(40) Mukhopadhyay, S.; Risko, C.; Marder, S. R.; Bredas, J.-L. Polymethine Dyes for All-Optical Switching Applications: A Quantum-Chemical Characterization of Counter-Ion and Aggregation Effects on the Third-Order Nonlinear Optical Response. *Chem. Sci.* **2012**, *3*, 3103−3112.
(41) Karton-Lifshin, N.; Albertazzi, L.; Bendikov, M.; Baran, P. S.; Shabat, D. "Donor−Two-Acceptor" Dye Design: A Distinct Gateway to NIR Fluorescence. *J. Am. Chem. Soc.* **2012**, *134*, 20412−20420.
(42) Yesudas, K. Cationic Cyanine Dyes: Impact of Symmetry-Breaking on Optical Absorption and Third-Order Polarizabilities. *Phys. Chem. Chem. Phys.* **2013**, *15*, 19465−19477.
(43) Thorley, K. J.; Hales, J. M.; Kim, H.; Ohira, S.; Brédas, J.-L.; Perry, J. W.; Anderson, H. L. Cyanine-like Dyes with Large Bond-Length Alternation. *Chem.—Eur. J.* **2013**, *19*, 10370−10377.
(44) Champagne, B.; Guillaume, M.; Zutterman, F. TDDFT Investigation of the Optical Properties of Cyanine Dyes. *Chem. Phys. Lett.* **2006**, *425*, 105−109.
(45) Guillaume, M.; Liégeois, V.; Champagne, B.; Zutterman, F. Time-Dependent Density Functional Theory Investigation of the Absorption and Emission Spectra of a Cyanine Dye. *Chem. Phys. Lett.* **2007**, *446*, 165−169.
(46) Jacquemin, D.; Zhao, Y.; Valero, R.; Adamo, C.; Ciofini, I.; Truhlar, D. G. Verdict: Time-Dependent Density Functional Theory "Not Guilty" of Large Errors for Cyanines. *J. Chem. Theory Comput.* **2012**, *8*, 1255−1259.
(47) The $C_\omega$ atom is localized far away from the Y substituent, and therefore, variable inductive effects due to the Y substituent on its chemical shift can be neglected. For all compounds, the corresponding signal was unambiguously assigned by 2D HMBC and HSQC experiments.
(48) Frisch, M. J.; Trucks, G. W.; Schlegel, H. B.; Scuseria, G. E.; Robb, M. A.; Cheeseman, J. R.; Scalmani, G.; Barone, V.; Mennucci, B.; Petersson, G. A.; et al.. *Gaussian 09*, revisions A.02 and C.01; Gaussian Inc.: Wallingford, CT, 2009.
(49) Runge, E.; Gross, E. K. U. Density-Functional Theory for Time-Dependent Systems. *Phys. Rev. Lett.* **1984**, *52*, 997−1000.
(50) Casida, M. E. Time-Dependent Density Functional Response Theory for Molecules, In *Recent Advances in Density Functional Methods*; Chong, D. P., Ed.; World Scientific: Singapore, 1995; Vol. *1*, pp 155−192.
(51) Tomasi, J.; Mennucci, B.; Cammi, R. Quantum Mechanical Continuum Solvation Models. *Chem. Rev.* **2005**, *105*, 2999−3094.
(52) Zhao, Y.; Truhlar, D. The M06 Suite of Density Functionals for Main Group Thermochemistry, Thermochemical Kinetics, Noncovalent Interactions, Excited States, and Transition Elements: Two New Functionals and Systematic Testing of Four M06-Class Functionals and 12 Other Functionals. *Theor. Chem. Acc.* **2008**, *120*, 215−241.
(53) Ernzerhof, M.; Scuseria, G. E. Assessment of the Perdew−Burke−Ernzerhof exchange-correlation functional. *J. Chem. Phys.* **1999**, *110*, 5029−5036.
(54) Adamo, C.; Barone, V. Toward Reliable Density Functional Methods without Adjustable Parameters: The PBE0 Model. *J. Chem. Phys.* **1999**, *110*, 6158−6170.
(55) Chai, J.-D.; Head-Gordon, M. Long-Range Corrected Hybrid Density Functionals with Damped Atom−Atom Dispersion Corrections. *Phys. Chem. Chem. Phys.* **2008**, *10*, 6615−6620.
(56) Cioslowski, J. A New Population Analysis Based on Atomic Polar Tensors. *J. Am. Chem. Soc.* **1989**, *111*, 8333−8336.
(57) Jacquemin, D.; Planchat, A.; Adamo, C.; Mennucci, B. TD-DFT Assessment of Functionals for Optical 0−0 Transitions in Solvated Dyes. *J. Chem. Theory Comput.* **2012**, *8*, 2359−2372.
(58) Charaf-Eddin, A.; Planchat, A.; Mennucci, B.; Adamo, C.; Jacquemin, D. Choosing a Functional for Computing Absorption and Fluorescence Band Shapes with TD-DFT. *J. Chem. Theory Comput.* **2013**, *9*, 2749−2760.
(59) Santoro, F.; Improta, R.; Lami, A.; Bloino, J.; Barone, V. Effective Method To Compute Franck−Condon Integrals for Optical Spectra of Large Molecules in Solution. *J. Chem. Phys.* **2007**, *126*, 084509.
(60) Santoro, F.; Lami, A.; Improta, R.; Barone, V. Effective Method To Compute Vibrationally Resolved Optical Spectra of Large Molecules at Finite Temperature in the Gas Phase and in Solution. *J. Chem. Phys.* **2007**, *126* (184102), 1−12.
(61) Piotto, M.; Bourdonneau, M.; Elbayed, K.; Wieruszeski, J.-M.; Lippens, G. New DEFT Sequences for the Acquisition of One-Dimensional Carbon NMR Spectra of Small Unlabelled Molecules. *Magn. Reson. Chem.* **2006**, *44*, 943−947.